FULL PAPER *Surgery*

Bone Regeneration by the Combined Use of Tetrapod-Shaped Calcium Phosphate Granules with Basic Fibroblast Growth Factor-Binding Ion Complex Gel in Canine Segmental Radial Defects

Muneki HONNAMI[1, 2], Sungjin CHOI[3], I-li LIU[1], Wataru KAMIMURA[4, 5], Tetsushi TAGUCHI[5], Hironori HOJO[3], Nobuyuki SHIMOHATA[3], Shinsuke OHBA[3], Hiroyuki KOYAMA[4], Ryohei NISHIMURA[6], Ung-il CHUNG[2, 3], Nobuo SASAKI[1] and Manabu MOCHIZUKI[1]*

[1]*Laboratory of Veterinary Surgery, Graduate School of Agricultural and Life Sciences, The University of Tokyo, 1–1–1 Yayoi, Bunkyo-ku, Tokyo 113–8657, Japan*

[2]*Department of Bioengineering, Graduate School of Engineering, The University of Tokyo, 7–3–1 Hongo, Bunkyo-ku, Tokyo 113–8655, Japan*

[3]*Division of Clinical Biotechnology, Center for Disease Biology and Integrative Medicine, Graduate School of Medicine, The University of Tokyo, 7–3–1 Hongo, Bunkyo-ku, Tokyo 113–8655, Japan*

[4]*Division of Tissue Engineering, Department of Vascular Regeneration, The University of Tokyo Hospital, 7–3–1 Hongo, Bunkyo-ku, Tokyo 113–8655, Japan*

[5]*Smart Biomaterials Group, Biomaterials Unit, Nanoscale Materials Division, National Institute for Materials Science, 1–1 Namiki, Tsukuba, Ibaraki 305–0044, Japan*

[6]*Laboratory of Veterinary Emergency Medicine, Graduate School of Agricultural and Life Sciences, The University of Tokyo, 1–1–1 Yayoi, Bunkyo-ku, Tokyo 113–8657, Japan*

(Received 14 January 2014/Accepted 11 March 2014/Published online in J-STAGE 26 March 2014)

ABSTRACT. The effect of tetrapod-shaped alpha tricalcium phosphate granules (Tetrabones® [TB]) in combination with basic fibroblast growth factor (bFGF)-binding ion complex gel (f-IC gel) on bone defect repair was examined. Bilateral segmental defects 20-mm long were created in the radius of 5 dogs, stabilized with a plate and screws and implanted with 1 of the following: TB (TB group), TB and bFGF solution (TB/f group), and TB and f-IC gel (TB/f-IC group). Dogs were euthanized 4 weeks after surgery. Radiographs showed well-placed TB granules in the defects and equal osseous callus formation in all the groups. Histomorphometry revealed that the number of vessels and volume of new bone in the TB/f-IC group were significantly higher than those in the other groups. However, no significant differences in neovascularization and new bone formation were observed between the TB/f and TB groups. Furthermore, no significant difference in the lamellar bone volume or rate of mineral apposition was observed among groups. These results suggest that increased bone formation might have been because of the promotion of neovascularization by the f-IC gel. Therefore, the combinatorial method may provide a suitable scaffold for bone regeneration in large segmental long bone defects.

KEY WORDS: bone regeneration, calcium phosphate, collagen, fibroblast growth factor, histomorphometry.

doi: 10.1292/jvms.14-0027; *J. Vet. Med. Sci.* 76(7): 955–961, 2014

Bioceramic materials, such as calcium phosphate ceramics, have been extensively used for bone defects, because of their biodegradability and osteoconductivity. However, the limitation of single use of calcium phosphate ceramics may be its lack of osteoinductivity. Therefore, the combined use of calcium phosphate ceramics with various growth factors and biocompatible scaffolds has been widely investigated [13, 14].

Blood supply plays a pivotal role in fracture healing [3, 4], and enhanced vascularity has been shown to facilitate bone regeneration [20, 21, 23]. In our previous study, we demonstrated that an ion complex gel (IC gel) consisting of collagen and a citric acid derivative induced the growth of highly vascular tissues into the gel after implantation into the subfascial space in rats, and the binding of the basic fibroblast growth factor (bFGF) to the IC gel (f-IC gel) further enhanced neovascularization [22]. We also fabricated calcium phosphate alpha tricalcium phosphate granules (called Tetrabones® [TB]), which are tetrapod shaped and 1 mm in size. When packed together, the TB form intergranular pores of an appropriate size (100–400 μm), interconnecting to facilitate cellular and vascular invasions [1].

Our recent study demonstrated that the combination of TB and f-IC gel facilitated neovascularization and new bone formation in rabbits with segmental femoral defects [5]. To predict its clinical efficacy in both veterinary and human medicine, a more elaborate histomorphological study using canines with a more closely related bone metabolism to that in humans is needed.

Therefore, the present study aimed at evaluating via bone morphometric analysis, the combination effect of TB and

*CORRESPONDENCE TO: MOCHIZUKI, M., Laboratory of Veterinary Surgery, Graduate School of Agricultural and Life Sciences, The University of Tokyo, 1–1–1 Yayoi, Bunkyo-ku, Tokyo 113–8657, Japan. e-mail: amm@mail.ecc.u-tokyo.ac.jp

f-IC gel on neovascularization and bone regeneration in canine segmental radial defects.

MATERIALS AND METHODS

Preparation of tetrapod-shaped alpha tricalcium phosphate granules (TB): The procedure used in the preparation of the TB was previously described [1], and the materials (Tetrabones®) were obtained from NEXT21, K.K. (Tokyo, Japan).

Preparation of bFGF-binding ion complex gel matrix (f-IC gel): The procedure used in the preparation of the f-IC gel was previously described [18, 19, 22]. Briefly, the IC gel formed spontaneously at room temperature by mixing the same volume of alkali-treated collagen modified with citric acid derivatives (CADs) and atelocollagen derived from pig tissues (Nitta Gelatin Inc., Osaka, Japan). Before gel formation, recombinant human bFGF (Kaken Pharmaceutical Co., Ltd., Tokyo, Japan) was added to the mixed solution at a final concentration of 100 *n*g/m*l*.

Animals and surgical procedures: All the animal experiments in this study were conducted in accordance with the guidelines of the Animal Care Committee of the Graduate School of Agricultural and Life Sciences at The University of Tokyo. Five male beagle dogs, aged 13–19 months and weighing 10.5–11.3 kg, were used in the experiment.

Intravenous propofol (8 mg/kg) was used to induce anesthesia, which was maintained using isoflurane (1.5–2.5%) in oxygen. Fentanyl hydrate (10–20 $\mu g \cdot kg^{-1} \cdot hr$) was administered as a constant-rate infusion throughout the surgery to induce analgesia. Lactated Ringer's solution (10 $ml \cdot kg^{-1} \cdot hr$) was infused, and intravenous cefazolin (20 mg/kg) was administered before the skin incision was made and every 2 hr thereafter. After sterilization, the radius shaft was exposed through a craniolateral skin incision, and a critically sized (20-mm long) mid-diaphyseal segmental defect [6] was created using an oscillating saw. A defect of the same size was created in each side of the radius. A polypropylene mesh cage (PMC), 9 mm in diameter and 28 mm in height, was fabricated to hold the TB granules in the defect, as previously described (Fig. 1) [5]. Then, the PMC containing the TB with or without the bFGF or f-IC gel was inserted to the defect and fixed with an 8-hole stainless bone plate 1.8 mm thick (custom-made buttress plate, Mizuho Co., Ltd., Tokyo, Japan) and 8 screws (φ2.7-mm stainless cortical screw, Synthes Vet, Tokyo, Japan). Both ends of the PMC were tucked between the plate and the intact bone ends. Then, the muscles, fascia lata and subcutaneous tissue were sutured. Cefazolin (20 mg/kg, subcutaneously twice a day) and buprenorphine (15 μg/kg, intramuscularly 3 times a day) were administered for 3 days after surgery. A Robert-Jones bandage was used in all the dogs 1 day after surgery.

Five dogs with 10 radial defects were included in this study and were randomly divided into the following groups: TB group (n=4), implanted with PMC and TB; TB/f group (n=3), implanted with PMC, TB (1.2 g) and bFGF solution (100 *n*g/m*l*, 1.0 m*l*); and TB/f-IC group (n=3), implanted with PMC, TB and f-IC gel (100 *n*g/m*l*, 1.0 m*l*). In the TB/f group, 100-*n*g/m*l* bFGF/phosphate-buffered saline solution was poured into the TB during surgery. The dogs in all the groups were euthanized 4 weeks after surgery.

Fluorescent bone labeling: The dogs were intravenously injected with oxytetracycline (TC; 20 mg/kg; Terramycin/LA, Pfizer Japan, Inc., Tokyo, Japan) 14 days after surgery and calcein (CL; 20 mg/kg; Sigma-Aldrich Co., Tokyo, Japan) 21 days after surgery.

Radiography and micro-computed tomography: Lateral radiographs were obtained immediately after surgery and upon euthanasia. After removing the metallic implants, with the PMC retained, micro-computed tomographic (micro-CT) images (SMX-90CT, Shimadzu Co., Kyoto, Japan) of the defects at the midsagittal sections were obtained.

Histomorphometry: The harvested radius was fixed with 70% ethanol for 5 days, stained with Villanueva bone stain for 7 days, dehydrated in ascending grades of ethanol, defatted in an acetone-methyl methacrylate monomer mixture (1:2) and embedded in methyl methacrylate (Wako Chemicals, Odawara, Japan) without decalcification. Histological sections of 40-μm thickness were cut along the midsagittal plane from the intact proximal and distal ends of the radius and defect. The specimens were examined microscopically (BX-53, Olympus Co., Tokyo, Japan) under natural and polarized light and on fluorescence microscopy. The histomorphometric measurements were made using a semiautomatic image analyzing system (System Supply, Ina, Japan). The standard bone histomorphometric nomenclature, symbols and units described in the report of the American Society for Bone and Mineral Research Histomorphometry Nomenclature Committee [16] were used. The ratios (100%) of bone distance-tissue distance (BD/TD), bone volume-tissue volume (BV/TV) and lamellar bone volume/bone volume (LBV/BV); the number of vessels/analysis area (N.Ve/mm^2) and mineral apposition rate (MAR, μm/day) were calculated for each sample. The BD/TD was calculated for each sample in the midline of the defect. The LBV/BV was calculated under polarized light. Lamellar bone was defined as the regular parallel alignment of collagen as distinguished from woven bone, which was defined as a haphazard organization of collagen fibers. N.Ve/mm^2 was calculated in 3 longitudinal areas (cranial, medial and caudal) of the defect. A 20-mm^2 rectangle (1 × 20 mm) in each area was analyzed. Vessels were defined as luminal structures containing red blood cells. Using fluorescence microscopy, the MAR was calculated by dividing the bone thicknesses between the pairs of lines marking the administration of the fluorescent bone markers TC and CL by the time intervals between the doses (TC-CL, days 14 and 21; CL-osteoid, days 21 and 28).

Statistical analysis: Results were expressed as mean ± standard deviation. Statistical analysis was performed using the StatView Version 5.01 software (SAS Institute Inc., Cary, NC, U.S.A.). Statistical differences were analyzed using one-way analysis of variance followed by the Tukey-Kramer test for multiple comparisons. Differences were considered statistically significant at $P<0.05$.

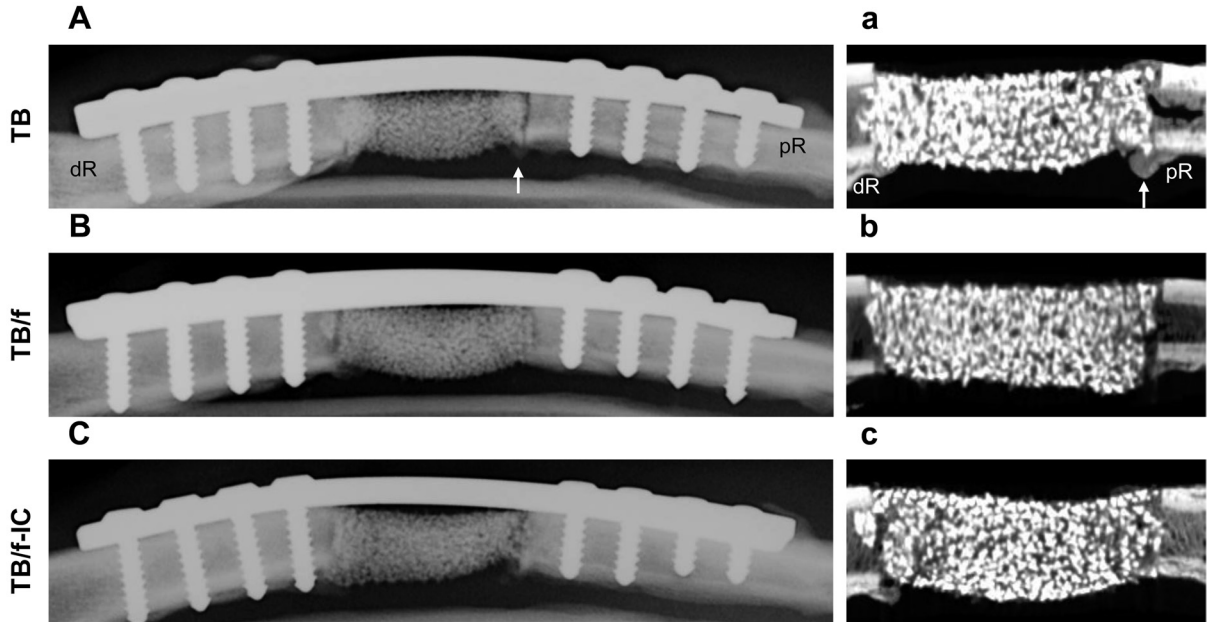

Fig. 2. (A–C) Radiographs and (a–c) micro-computed tomographic images of the radial segmental bone defects in each treatment group 4 weeks after surgery. (A, a) TB group; (B, b) TB/f group; and (C, c) TB/f-IC group. The arrows indicate the osseous callus formation extending from the intact proximal bone cortex over the defect. dR: distal radius, pR: proximal radius.

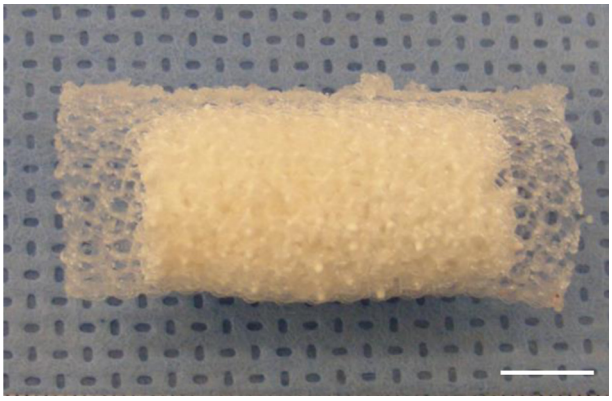

Fig. 1. (A) Tetrabones® (TB)-containing polypropylene mesh cage (PMC). The TB was packed into the PMC. Both ends of the PMC were tucked between the plate and intact bone ends. Scale bar=500 μm.

RESULTS

Surgical outcome and clinical findings: Macroscopically, the defect and PMC were stabilized well using a plate and screws without TB leakage during the surgery. All the dogs tolerated the surgical procedures and had a complete, uneventful recovery.

Radiological findings: The plain radiographs (Fig. 2A–2C) and micro-CT images (Fig. 2a–2c) showed that the TB granules were placed in the defects without leakage but with slight caudal displacement of the middle portion of the TB.

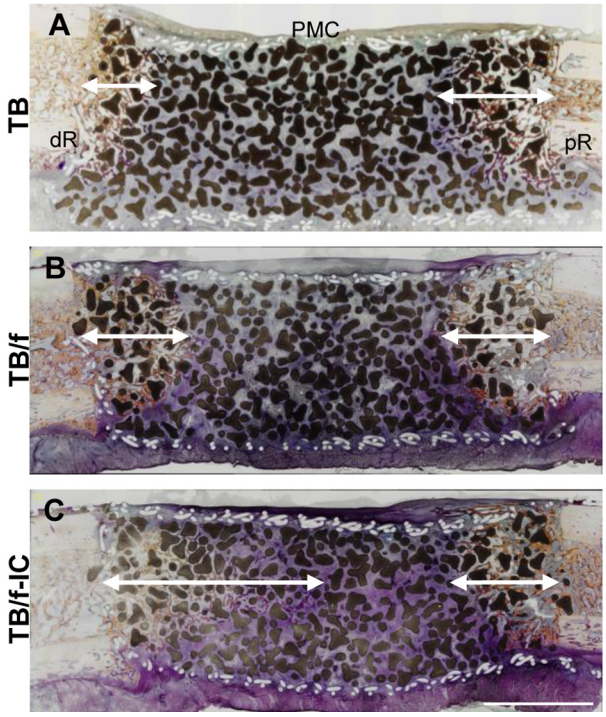

Fig. 3. (A–J) Histological sections (Villanueva bone stain) at the midsagittal plane of the TB (A), TB/f (B) and TB/f-IC groups (C) 4 weeks after surgery. dR: distal radius, pR: proximal radius, PMC: polypropylene mesh cage. The arrows indicate the distance of the distal and proximal new bone tissues from the midline of the defect. Scale bar=5 mm.

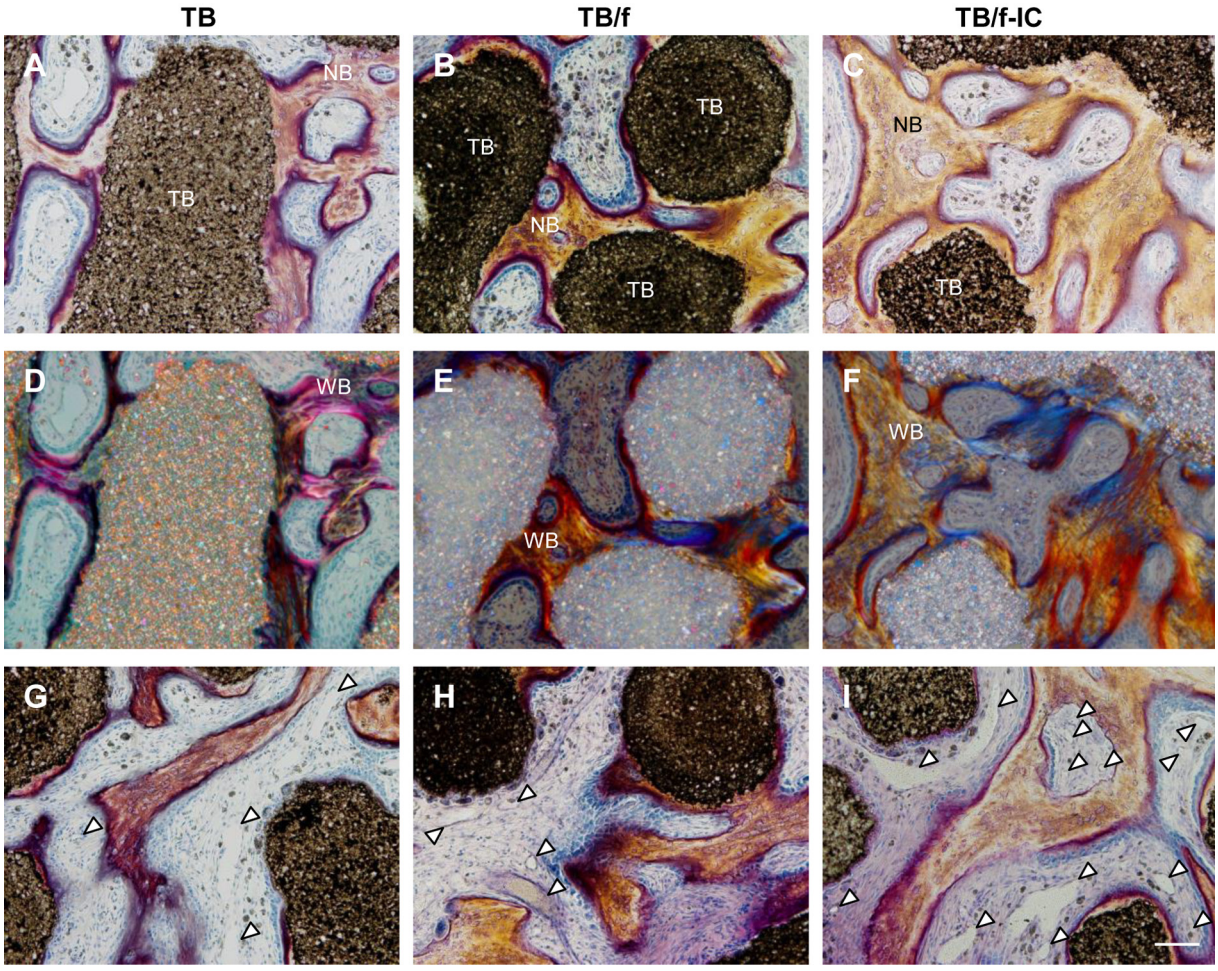

Fig. 4. Histological findings of newly formed bone (A–C: natural light, D–F: polarized light) and neovascularization (G–I: natural light) in the TB (A, D and G), TB/f (B, E and H) and TB/f-IC groups (C, F and I) 4 weeks after surgery. TB: Tetrabones, NB: new bone, WB: woven bone. The arrowheads indicate the newly formed vessels. Scale bar=200 μm.

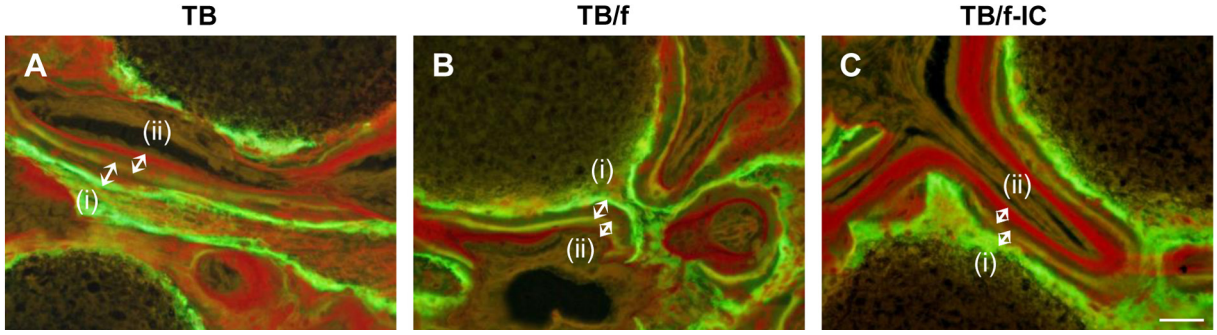

Fig. 5. Histological findings of fluorescently labeled newly formed bone. The yellow and green lines indicate the tetracycline and calcein signals, respectively, in the TB (A), TB/f (B) and TB/f-IC groups (C) 4 weeks after surgery: the thicknesses (i) from day 14 to 21 and (ii) from day 21 to 28. Scale bar=50 μm.

Although it was difficult to distinguish the newly formed bone in the intergranular pores of the TB, osseous callus formation extending from the intact bone cortex over the implant was observed 4 weeks after surgery in each group.

Histomorphometric findings: Figure 3 shows the histological sections for each group. In the TB/f-IC group, more

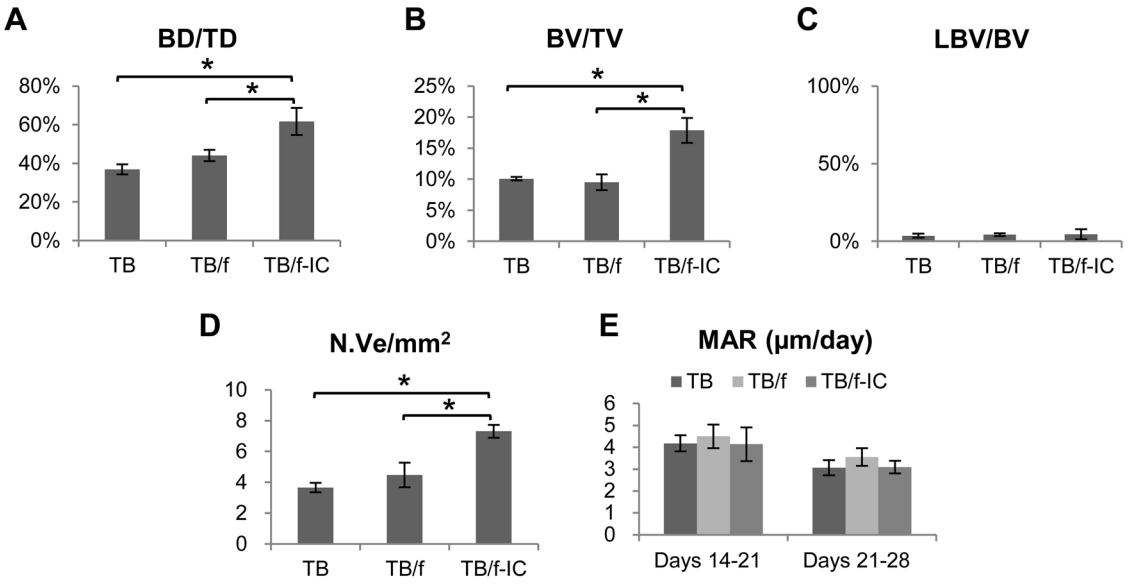

Fig. 6. Results of the histomorphometric analyses of the newly formed bone 4 weeks after surgery. (A) The distances of the proximal and distal new bone tissues per total tissue distance (BD/TD), (B) the volume of bone tissue per volume of total tissue (BV/TV), (C) the volume of lamellar bone tissue per volume of bone tissue (LBV/BV), (D) the number of vessels per square millimeter (N.Ve/mm^2) and (E) the mineral apposition rate (MAR). Values are shown as mean ± standard deviation. The asterisks indicate statistically significant differences between the groups (one-way analysis of variance followed by the Tukey-Kramer test for multiple comparison; $P<0.05$).

newly formed bone was observed, especially from the distal radius, compared with that in the TB and TB/f groups. Figure 4 shows the histological findings from the defect in each group. As shown in Fig. 4A–4C, the histological sections under natural light revealed more extensive bone formation in the TB/f-IC group than in the TB and TB/f groups. Detailed analysis of the histological sections under polarized light revealed that the newly formed bone in each group mainly consisted of woven bone (Fig. 4D–4F). Furthermore, more neovascularization was observed in the TB/f-IC group than in the TB and TB/f groups (Fig. 4G–4I). Figure 5 shows the histological sections of the fluorescence-labeled newly formed bone with TC (yellow lines) and CL (green lines) signals in each group. The mineral apposition during certain periods after implantation was analyzed by examining the incorporation of the fluorescence labels, TC and CL, into the bones. The bone thicknesses of the 2 pairs of lines, TC-CL and CL-osteoid, did not differ grossly among the groups (Fig. 5).

Figure 6 shows the results of the histomorphometry using the histological findings in Figs. 4 and 5. As shown in Fig. 6 (A, B and D), BD/TD, BV/TV and N.Ve/mm^2 were significantly higher in the TB/f-IC group than in the other groups 4 weeks after surgery. The values of BD/TD, BV/TV and N.Ve/mm^2 in the TB/f-IC group were 61.6 ± 7.0%, 17.9 ± 2.0% and 7.3 ± 0.4, respectively; however, no significant differences in these 3 parameters were found between the TB/f and TB groups. The values of BD/TD, BV/TV and N.Ve/mm^2 in the TB versus TB/f group were 36.9 ± 2.6% versus 44.1 ± 2.9%, 10.1 ± 0.3% versus 9.5 ± 1.3% and 3.7 ± 0.3 versus 4.5 ± 0.8, respectively. As shown in Fig. 6 (C and E), no significant differences in LBV/BV and MAR values were observed between the groups.

DISCUSSION

In our recent study, the combination of TB and f-IC gel facilitated neovascularization and new bone formation in a rabbit segmental femoral defect model [5]. The results also demonstrated that the combination successfully facilitated neovascularization and new bone formation within 4 weeks after surgery in critically sized (20 mm) segmental radial defects in dogs.

In the present study, the number of vessels in the defects in the TB/f-IC group was significantly higher than that in the TB and TB/f groups, whereas no significant difference was found between the TB and TB/f groups. These results suggest that the f-IC gel induced angiogenic effects in the dogs. Our previous studies demonstrated that the IC gel alone markedly induced vessel growth and that its combined use with bFGF significantly enhanced the vascularization ability of the IC gel in rats [22] and rabbits [5]. Furthermore, the enhanced neovascularization in the TB/f-IC group was accompanied by a significantly greater ingrowth of newly formed bone than that in the TB and TB/f groups, suggesting that the increased formation of new bone might be because of the promotion of neovascularization by the f-IC gel.

The IC gel was developed as an extracellular matrix (ECM)-like scaffold [22]. Vessels produced in the defect were essentially within the ECM, which functioned as a

natural scaffold for the vessel structure. The IC gel has a stable three-dimensional matrix structure and is degradable to develop vascular network by a variety of proteases generally released from vascular cells and related cells. Another crucial feature of the IC gel is that it serves as a reservoir of the bFGF as an angiogenic factor. Given that bFGF is positively charged and the CAD part of the IC gel is negatively charged, the bFGF can bind to the CAD with ionic bonds, fixing itself inside the IC gel. Therefore, the bFGF stimulates neovascularization and accelerates the development of a vascular network in the gel. The concentration of bFGF (100 *n*g/m*l*) in the IC gel used in this study was the minimum level required to achieve the full effect on neovascularization [22].

bFGF is known as an osteoinductive factor [2, 17] and has been demonstrated at a single local application (100–200 μg/site) to produce osteoinduction in animal bone defects or fracture models in several species including rats, rabbits, dogs and nonhuman primates [9, 11, 12, 15]. Kawaguchi *et al.* [10] reported that the bFGF at high concentrations acted on osteoblastic cells and stimulated not only bone formation but also bone resorption. Recent studies demonstrated that using a low dose of the bFGF (rabbits, 1.4 μg/site; dogs, 0.15 μg/site) combined with collagen minipellets as a drug delivery system successfully facilitated bone regeneration in femoral segmental defects in rabbits and guided bone regeneration (GBR) sites in dogs [7, 8]. Although the bFGF dose (100 *n*g/site) in this study was much lower than that used in previous studies, the f-IC gel in this study successfully facilitated bone regeneration via the binding of the bFGF to the IC gel with ionic bonds.

In addition, the f-IC gel was compatible with various granular artificial bones, in contrast to the collagen minipellets. The TB used in this study consisted of 1-mm tetrapod-shaped granules and formed intergranular pores of an appropriate size (100–400 μm), interconnecting to facilitate cellular and vascular invasions when packed together [1]. Therefore, the combination of the TB and f-IC gel may provide an ideal scaffold for bone regeneration in large bone defects that require an osteoconductive scaffold and vascular network.

In this study, we calculated the LBV/BV and MAR to precisely evaluate the osteoinductive effect of the low-dose bFGF in the IC gel. The LBV/BV value indicates the percentage of remodeling area occupied by newly formed bone and is supposed to reflect an aspect of the bone healing process in which initially formed bone, woven bone, is gradually replaced by lamellar bone through cooperative actions of osteoblasts and osteoclasts. Meanwhile, the MAR value indicates the linear rate of production of calcified bone matrix by the osteoblasts. The present study demonstrated that neither the LBV/BV nor MAR values differed significantly among the groups, suggesting that the IC gel in combination with the bFGF facilitated increased bone regeneration through neovascularization rather than by enhancing bone turnover, although the bFGF within the IC gel might have also contributed to bone regeneration. However, longer observation periods than 4 weeks are needed to get more precisely evaluation of bone turnover, because lamellar bone appears relatively late phase of the bone healing process.

In conclusion, the present study revealed that the combination of tetrapod-shaped alpha tricalcium phosphate granules and the f-IC gel facilitated bone regeneration by inducing neovascularization in a canine segmental radial defect model. This combination may be a clinically suitable scaffold for the treatment of segmental long bone defects. However, additional long-term studies are necessary to predict its clinical efficacy.

ACKNOWLEDGMENTS. This work was supported by the Japan Society for the Promotion of Science (JSPS) through the Grants-in-Aid for Scientific Research, the Center for Medical System Innovation (CMSI), the Graduate Program for Leaders in Life Innovation (GPLLI), the International Core Research Center for Nanobio, Core-to-Core Program, A. Advanced Research Networks and the Funding Program for World-Leading Innovative R&D on Science and Technology (FIRST program); the Ministry of Education, Culture, Sports, Science and Technology in Japan (MEXT) through the Center for NanoBio Integration (CNBI); the Japan Science and Technology Agency (JST) through the S-innovation program; and the Research and Development Programs for Three-dimensional Complex Organ Structures and for Autonomous Regeneration Devices from the New Energy and Industrial Technology Development Organization (NEDO).

We sincerely thank Dr. Akemi Ito, Ito Bone Histomorphometry Institute, Niigata, Japan, for her invaluable assistance.

REFERENCES

1. Choi, S., Liu, I. L., Yamamoto, K., Igawa, K., Mochizuki, M., Sakai, T., Echigo, R., Honnami, M., Suzuki, S., Chung, U. I. and Sasaki, N. 2012. Development and evaluation of tetrapod-shaped granular artificial bones. *Acta Biomater.* **8**: 2340–2347. [Medline] [CrossRef]
2. Globus, R. K., Patterson-Buckendahl, P. and Gospodarowicz, D. 1988. Regulation of bovine bone cell proliferation by fibroblast growth factor and transforming growth factor beta. *Endocrinology* **123**: 98–105. [Medline] [CrossRef]
3. Glowacki, J. 1998. Angiogenesis in fracture repair. *Clin. Orthop. Relat. Res.* S82–S89. [Medline] [CrossRef]
4. Hankenson, K. D., Dishowitz, M., Gray, C. and Schenker, M. 2011. Angiogenesis in bone regeneration. *Injury* **42**: 556–561. [Medline] [CrossRef]
5. Honnami, M., Choi, S., Liu, I. L., Kamimura, W., Taguchi, T., Hojo, H., Shimohata, N., Ohba, S., Koyama, H., Nishimura, R., Chung, U. I., Sasaki, N. and Mochizuki, M. 2013. Repair of rabbit segmental femoral defects by using a combination of tetrapod-shaped calcium phosphate granules and basic fibroblast growth factor-binding ion complex gel. *Biomaterials* **34**: 9056–9062. [Medline] [CrossRef]
6. Horner, E. A., Kirkham, J., Wood, D., Curran, S., Smith, M., Thomson, B. and Yang, X. B. 2010. Long bone defect models for tissue engineering applications: criteria for choice. *Tissue Eng. Part B Rev.* **16**: 263–271. [Medline] [CrossRef]
7. Hosokawa, R., Kikuzaki, K., Kimoto, T., Matsuura, T., Chiba, D., Wadamoto, M., Sato, Y., Maeda, M., Sano, A. and Akagawa, Y. 2000. Controlled local application of basic fibroblast growth

factor (FGF-2) accelerates the healing of GBR. An experimental study in beagle dogs. *Clin. Oral Implants Res.* **11**: 345–353. [Medline] [CrossRef]
8. Inui, K., Maeda, M., Sano, A., Fujioka, K., Yutani, Y., Sakawa, A., Yamano, Y., Kato, Y. and Koike, T. 1998. Local application of basic fibroblast growth factor minipellet induces the healing of segmental bony defects in rabbits. *Calcif. Tissue Int.* **63**: 490–495. [Medline] [CrossRef]
9. Kato, T., Kawaguchi, H., Hanada, K., Aoyama, I., Hiyama, Y., Nakamura, T., Kuzutani, K., Tamura, M., Kurokawa, T. and Nakamura, K. 1998. Single local injection of recombinant fibroblast growth factor-2 stimulates healing of segmental bone defects in rabbits. *J. Orthop. Res.* **16**: 654–659. [Medline] [CrossRef]
10. Kawaguchi, H., Chikazu, D., Nakamura, K., Kumegawa, M. and Hakeda, Y. 2000. Direct and indirect actions of fibroblast growth factor 2 on osteoclastic bone resorption in cultures. *J. Bone Miner. Res.* **15**: 466–473. [Medline] [CrossRef]
11. Kawaguchi, H., Kurokawa, T., Hanada, K., Hiyama, Y., Tamura, M., Ogata, E. and Matsumoto, T. 1994. Stimulation of fracture repair by recombinant human basic fibroblast growth factor in normal and streptozotocin-diabetic rats. *Endocrinology* **135**: 774–781. [Medline]
12. Kawaguchi, H., Nakamura, K., Tabata, Y., Ikada, Y., Aoyama, I., Anzai, J., Nakamura, T., Hiyama, Y. and Tamura, M. 2001. Acceleration of fracture healing in nonhuman primates by fibroblast growth factor-2. *J. Clin. Endocrinol. Metab.* **86**: 875–880. [Medline] [CrossRef]
13. Komaki, H., Tanaka, T., Chazono, M. and Kikuchi, T. 2006. Repair of segmental bone defects in rabbit tibiae using a complex of β-tricalcium phosphate, type I collagen, and fibroblast growth factor-2. *Biomaterials* **27**: 5118–5126. [Medline] [CrossRef]
14. Liu, B. and Lun, D. X. 2012. Current application of beta-tricalcium phosphate composites in orthopaedics. *Orthop. Surg.* **4**: 139–144. [Medline] [CrossRef]
15. Nakamura, T., Hara, Y., Tagawa, M., Tamura, M., Yuge, T., Fukuda, H. and Nigi, H. 1998. Recombinant human basic fibroblast growth factor accelerates fracture healing by enhancing callus remodeling in experimental dog tibial fracture. *J. Bone Miner. Res.* **13**: 942–949. [Medline] [CrossRef]
16. Parfitt, A. M., Drezner, M. K., Glorieux, F. H., Kanis, J. A., Malluche, H., Meunier, P. J., Ott, S. M. and Recker, R. R. 1987. Bone histomorphometry: standardization of nomenclature, symbols, and units. Report of the ASBMR Histomorphometry Nomenclature Committee. *J. Bone Miner. Res.* **2**: 595–610. [Medline] [CrossRef]
17. Rodan, S. B., Wesolowski, G., Thomas, K. A., Yoon, K. and Rodan, G. A. 1989. Effects of acidic and basic fibroblast growth factors on osteoblastic cells. *Connect. Tissue Res.* **20**: 283–288. [Medline] [CrossRef]
18. Saito, H., Murabayashi, S., Mitamura, Y. and Taguchi, T. 2007. Unusual cell adhesion and antithrombogenic behavior of citric acid-cross-linked collagen matrices. *Biomacromolecules* **8**: 1992–1998. [Medline] [CrossRef]
19. Saito, H., Taguchi, T., Aoki, H., Murabayashi, S., Mitamura, Y., Tanaka, J. and Tateishi, T. 2007. pH-responsive swelling behavior of collagen gels prepared by novel crosslinkers based on naturally derived di- or tricarboxylic acids. *Acta Biomater.* **3**: 89–94. [Medline] [CrossRef]
20. Stewart, R., Goldstein, J., Eberhardt, A., Gabriel Chu, G. T.M. and Gilbert, S. 2011. Increasing vascularity to improve healing of a segmental defect of the rat femur. *J. Orthop. Trauma* **25**: 472–476. [Medline] [CrossRef]
21. Street, J., Bao, M., deGuzman, L., Bunting, S., Peale, F. V., Ferrara, N., Steinmetz, H., Hoeffel, J., Cleland, J. L., Daugherty, A., van Bruggen, N., Redmond, H. P., Carano, R. A. D. and Filvaroff, E. H. 2002. Vascular endothelial growth factor stimulates bone repair by promoting angiogenesis and bone turnover. *Proc. Natl. Acad. Sci. U.S.A.* **99**: 9656–9661. [Medline] [CrossRef]
22. Takayama, T., Taguchi, T., Koyama, H., Sakari, M., Kamimura, W., Takato, T., Miyata, T. and Nagawa, H. 2009. The growth of a vascular network inside a collagen-citric acid derivative hydrogel in rats. *Biomaterials* **30**: 3580–3587. [Medline] [CrossRef]
23. Wang, L., Fan, H., Zhang, Z. Y., Lou, A. J., Pei, G. X., Jiang, S., Mu, T. W., Qin, J. J., Chen, S. Y. and Jin, D. 2010. Osteogenesis and angiogenesis of tissue-engineered bone constructed by prevascularized β-tricalcium phosphate scaffold and mesenchymal stem cells. *Biomaterials* **31**: 9452–9461. [Medline] [CrossRef]